Technical Report TR-2017-01

An Overview of the Chrono Soil Contact Model (SCM) Implementation

Alessandro Tasora, Dario Mangoni, Dan Negrut

Version: January 3, 2017

Abstract

This document contains details of the SCM deformable soil model implemented in Chrono. The soft soil model discussed herein is an extended version of the classical SCM Soil Contact Model used at DLR for predicting rover mobility. The model, which is based on a fast semi-empirical expeditious approach that requires few parameters, is ideal for scenarios that require a fast (near real-time) simulation of wheeled/tracked vehicle interaction with soft soils. For wheeled vehicles, no assumption is made regarding the wheel, which can be equipped with a deformable tire model.

Keywords: Semi empirical soil model, Deformable soil, Chrono, Vehicles, Tires

Contents

1 Introduction **3**

2 The SCM soil model **4**

3 Discretization **8**

4 Mesh refinement **9**

5 Conclusion **11**

1 Introduction

Many contact models have been developed for the tire/terrain interaction during the last fifty years. Most numerical approaches to the simulation of deformable soil fall into two categories: semi-empirical models and physics-based models.

Semi-empirical models, which are of relevance herein, are based on a small number of parameters that can be easily obtained experimentally. Given these soil strength parameters, pressure in the contact patch and traction performance are predicted using empirical relations based on approximate stress distributions that draw on various assumptions that make the problem tractable with simple analytical expressions. In general, these methods compute pressure and traction as outputs, given wheel sinkage as input.

Seminal contributions in the field of semi-empirical models have been made by Bekker in the 1950s – he developed equations that allowed the computation of the pressure field under a wheel traveling over a homogeneous deformable soil [3]. The Bekker model is interesting because it requires a minimal set of parameters for the characterization of the soil. During the years, the number of experimental tests for recovering those values has grown steadily to include today many different terrains. Remarkably, these parameters constitute the basis for many semi-empirical models have been developed in the following years.

In [24,25], the original Bekker model has been extended by Wong and Reece, to encompass more realistic shear effects. One of the most used assumptions for the shear forces is the one put forward in [8]. Here the draw-bar pull becomes a function of slip, thanks to an empirical function that relates shear and tangential displacement, tending to an horizontal asymptote. This model draws on the Mohr-Coulomb failure criterion augmented with an additional parameter k, referred to as the Janosi-Hanamoto shear modulus. Further research on this topic lead to more accurate models, for instance [19].

Recently, with new impetus generated by the interest in exploration of extraterrestrial bodies by means of autonomous rovers, many researchers focused on more accurate semi-empirical models and tried to generalize the original Wong-Reece model. The original Wong-Reece model is inherently 2D, but considering 3D effects in the soil model is important when one wants to simulate vehicles that perform complex maneuvers with short-radius steering. Along this line, the work of [4,7] presents a semi-empirical model that is capable of computing lateral forces caused by steering and lateral bulldozing; in this context the lateral bulldozing model is based on the simple blade model of [16].

Another approach that is capable of 3D effects is presented in [5, 12]. This model, called SCM in the following, is used as a basis for the formulation presented herein. It considers the soil as a height-map, thus the deformation produces a vertical displacement of the vertexes of a mesh.

The model presented in [1, 2] is based on fewer empirical assumptions because it directly applies the theory of plasticity to the soil using Drucker-Prager constitutive relation with cap hardening. Parameters are the same used in the classic theory of continuum elasto-plasticity. Nonetheless, the soil is represented as a simple height field, so it retains some attractive aspects of the models discussed above, for instance fast execution.

In literature there are many other contributions that have been made in the area of semi-empirical and fast models, among the many others we mention [6, 21] that address materials with low cohesion, [20] that consider the effect of multiple passes and soil surcharge at the side of the ruts, and [9] that discusses the effect of lugs.

Theoretical models, on the other side, aim at simulating the real physical phenomena at the interface of the tire an terrain by using complex, more computationally demanding, numerical approaches. At the cost of much higher CPU overhead, in general these approaches lead to more detailed results and they do not suffer the limitations of semi-empirical models. Moreover, they do not rely on empirical parameters, because they use the same material properties that would be used in finite element analyses. Among the various approaches presented in literature, we mention the use of Discrete Element Method for the soil, both with rigid wheels [14, 27] or with deformable FEA tires [15, 23] , or the use of FEA soil with elasto-plastic continuum coupled with FEA tires [26]. An alternative to using DEM is the non-smooth dynamics approach, based on Differential Variational Inequalities (DVI), discussed in [13, 22]. In the following section we will discuss the SCM model and how it has been extended and implemented in the Chrono multi-physics software.

2 The SCM soil model

The deformable soil model is derived from the model developed at the DLR and documented in [5,10–12,18]. The SCM model is based on a semi-empirical model with few parameters, as such it is easy to adjust and fast to simulate. In detail, it can be considered a generalization of the Bekker-Wong model to the case of wheels (or track shoes) with arbitrary three-dimensional shapes. We recall the Bekker formula for a wheel that moves on a deformable soil: the pressure-sinkage relationship is given by

$$\sigma = \left(\frac{k_c}{b} + k_\phi \right) y^n \tag{1}$$

where p is the contact patch pressure, y is wheel sinkage, k_c is an empirical coefficient representing the cohesive effect of the soil, k_ϕ is an empirical coefficient representing the stiffness of the soil, n is the exponent of sinkage, expressing the hardening effect in the soil compaction. Finally, according to Bekker, b is the length of the shorter side of the rectangular contact area. In fact this original Bekker model assumes a perfectly cylindrical tire in contact with a flat ground.

Following [12], we extend this to the case of a generic contact patch. For the generic patch, the b parameter cannot be interpreted as in the original Bekker model; one solution is shown by the algorithm presented in [12], another solution is to neglect completely the b parameter as in real scenarios, especially for moderate sinking hence with small vertical shear deformation in the soil, the effect of b on final results is often irrelevant.

Therefore we assume the soil to be a 3D continuum with $y(x, z)$ deformation along the vertical Y direction, as depicted in Fig.1. The initial shape of the soil y_0 needs not to be flat.

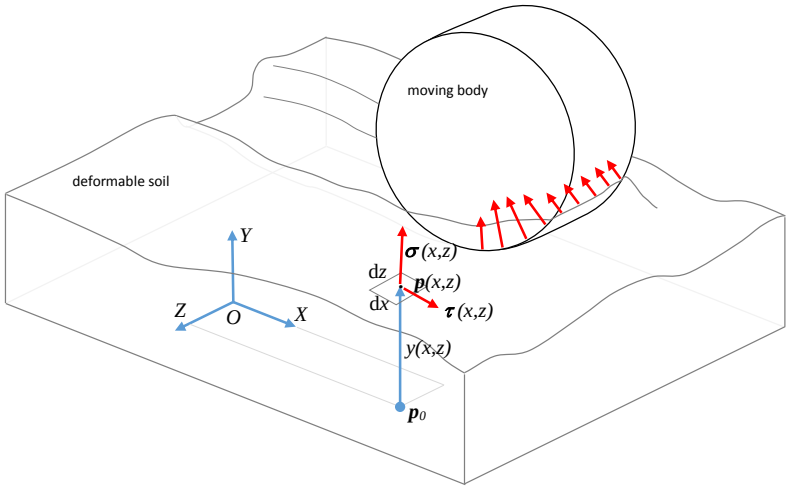

Figure 1: The deformable soil continuum.

As shown in Fig.2, under the effect of a moving (rolling or sliding) shape above it, the soil deforms and gets a permanent plastic deformation.

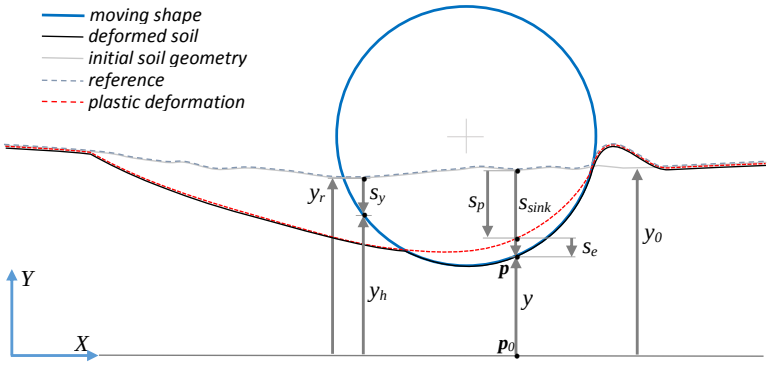

Figure 2: Deformation of the soil: variables used in formulas.

We assume that for whatever point $\mathbf{p}_0(x, y)$ on a global horizontal plane, it is possible to compute the elevation of the incoming moving shape by performing a ray-hit test from $\mathbf{p}_0(x, y)$ along $\mathbf{Y}$ up to the shape. The distance of the shape along $\mathbf{Y}$ is denoted y_h; if no shape is met, a fall-back large value $y_h = \epsilon_\infty$ is used.

One can compute s_y, the impressed deformation to the soil (as "sinking", we assume positive for downward deformation), as

$$s_y = y_r - y_h \tag{2}$$

where y_r is the initial reference height of the undeformed soil, something that depends for example on GIS data or user-provided 3D maps.

We note that at this point we are developing a rheological model where the pressure and sinking of each (x, z) point is independent on the state of all other points (something that in the original Bekker formula is accounted by the b coefficient). This is clearly a simplification of the real soil, because for example a point-based constitutive model cannot express vertical shear resistance, for example, but as we stated in the beginning, we must trade this approximation for the benefit of having a real-time final algorithm where one does not need to solve any linear system; moreover this locality assumption still gives precise results in many scenarios, especially for moderate sinking as we already said.

A major departure from the Bekker-Wong model, also discussed in [5], is the fact that the Bekker formula represents a purely plastic soil, without any elastic term. Although this is sufficient for most soils, it turns out that the lack of elastic terms can become a major source of troubles from the numerical point of view.

In fact, looking at Fig.3, one can see that a typical loading cycle goes from 0 to 1 along the soil hardening curve. The problem is that during a multibody simulation the sinking along s_y is not monotone (the vehicle can wobble, oscillate, jump) and, for the perfect plasticity, the reverse unloading goes from 1 to 2, then to whatever point 3, and when the tire touches again the soil, it goes again to 4 and 5, with the last computed pressure, and proceeds upward to 6 etc. One can see that the discontinuity from zero pressure in 4 to last yield pressure in 5 has a negative effect on the stability of the time integrator, and using stiff integrators is not always a remedial. It is enough that one unloads from 2 to 3 by an imperceptible s_y (ex. because of numerical noise) and this steep pattern is triggered. The side effect, in particular, it that a steady vehicle cannot sit steadily on the tire footprints as the contact pressures might be continuously switched on and off (i.e. like going from 4 to 5 and back, at each step).

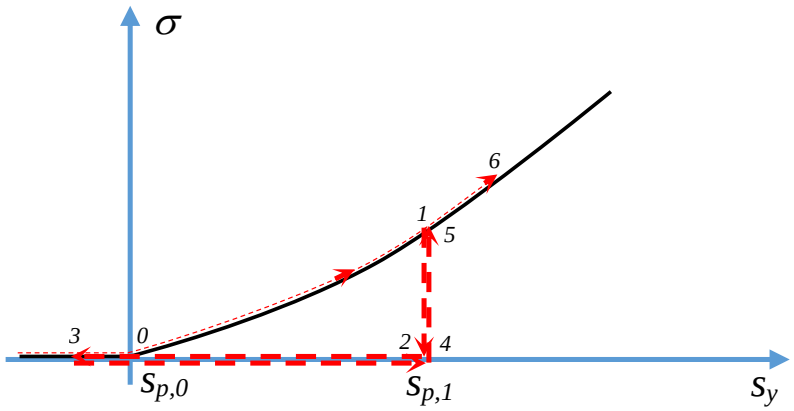

Figure 3: Purely plastic Bekker soil.

A solution is, then, to use a constitutive model that considers an elastic part, as in Fig.4. This allows a much more stable simulation in a context of multi-body time integration. The only drawback is that it requires an additional term, called k_e, that expresses the elastic stiffness of the soil. For $k_e \uparrow \infty$ and for coincident 0 and 1, the model still becomes the

original Bekker curve. Looking at Fig.4, one can see that the departure from the contact is never an abrupt on-off pattern, but rather descends from 2 to 3 in a continuous way, and the same when the contact is restored, from 4 to 5 and 6, and so on for further cycles. The unloading, as shown at the point 7, can also stop at a non-zero pressure level. This, averaged for the many contact points, is the model that we experienced to have the best numerical properties, it fixes all issues with vehicles not moving on steady ruts, and still inherits much of the original Bekker model.

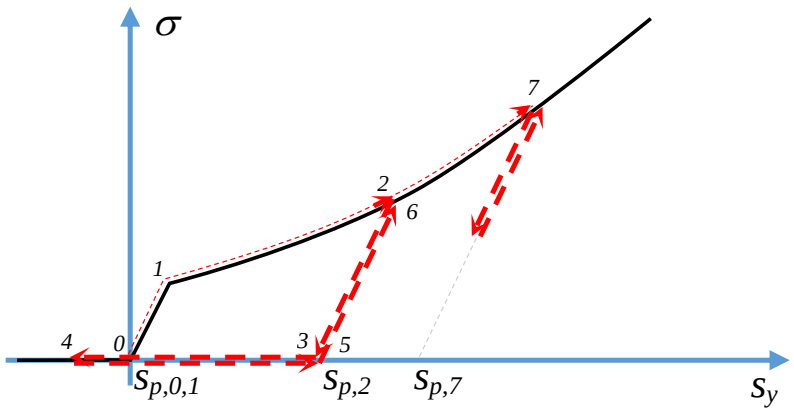

Figure 4: Elasto-plastic soil.

We proceed by assuming an elasto-plastic behavior of the soil, and we make the Reuss-Prandtl assumption

$$\dot{s}_y = \dot{s}_p - \dot{s}_e \tag{3}$$

where $\dot{s}_p$ is the plastic flow for the plastic sinking s_p and s_e is the elastic deformation.

By default the soil is initialized with $s_p = 0$ everywhere, but one could also provide a map of pre-compressed regions of soil where $s_p > 0$.

The algorithm for the computation of σ operates as follows.

A test pressure is computed as

$$\sigma_{try} = k_e(s_y - s_p) \tag{4}$$

If $\sigma_{try} \leq 0$ it violates the unilateral contact condition, so one simply returns $\sigma = 0$, and it keeps unaltered the deformation of the soil as $\dot{s}_p = 0$, $y = y_p$.

If $\sigma_{try} > 0$, we compute

$$\sigma^* = \sigma_{try} \tag{5}$$

$$s_{sink} = s_y \tag{6}$$

$$y = y_h \tag{7}$$

Also, the positive σ^* is clamped against the yield limit given by the plastic rule: if $\sigma^* < \sigma_{yeld}$ then it simply returns $\sigma = \sigma^*$, but if $\sigma^* > \sigma_{yeld}$ one computes for time-step h:

$$\sigma = k_\phi s_y^n \tag{8}$$

$$\sigma_{yeld} = \sigma \tag{9}$$

$$s_p^o = s_p \tag{10}$$

$$s_p = s_{sink} - \sigma / k_e \tag{11}$$

$$\dot{s}_p = (s_p - s_p^o)\frac{1}{h} \tag{12}$$

$$s_e = s_{sink} - s_p \tag{13}$$

Note that we did not use the Reuss-Prandtl formula directly, but we unrolled it to simplify the time integration of the plastic flow.

Optionally, one can also introduce a viscous damping effect, by updating

$$\sigma_{tot} = \sigma + v_n r \tag{14}$$

where r is a damping parameter and v_n is the modulus of the speed of compression of the soil.

3 Discretization

A discrete version of the above soil model is implemented, in order to perform the ray-hit test in a countable number of points. The original SCM model uses rectangular structured grids based on quadrilaterals, as in Fig.5. This is practical and fast, but we experienced that there are cases (especially large scenarios with long roads) where it could be useful to use unstructured grids. For this reason, our implementation supports unstructured meshes made with triangles, as in Fig.6.

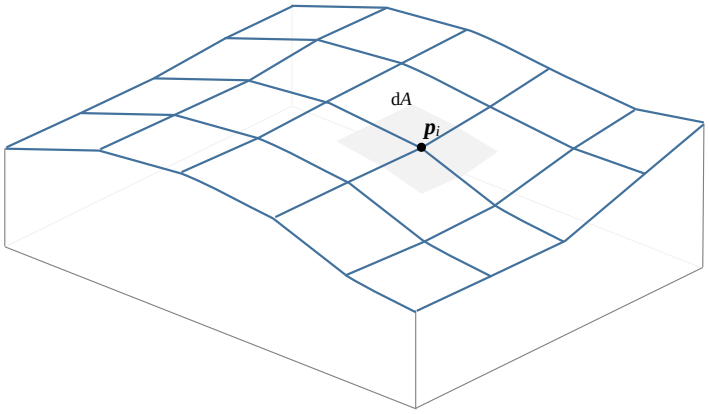

Figure 5: The original SCM soil, based on uniform structured grids.

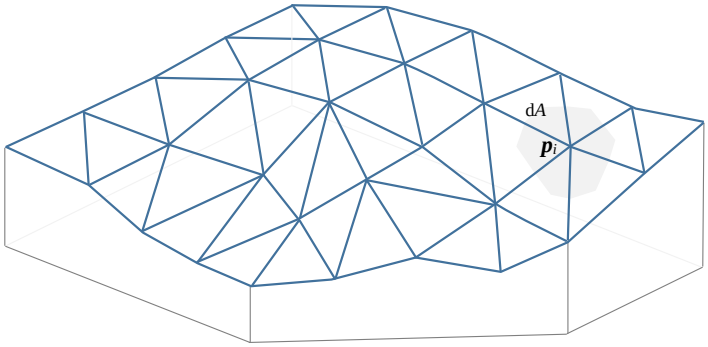

Figure 6: The modified SCM soil, based on unstructured triangular grids.

This means that, whereas one computes, say, the total vertical force as $F_y = \int_A \sigma_y dA = \sum_i (\sigma_{y,i} w_j)$ where $w_i = \Delta_x \Delta_z$ is the area of the i-th quadrilateral element of a grid with spacing Δ_x by Δ_z, and $\sigma_{y,i}$ is the pressure computed at that element, in our case one uses a modified formula that supports triangles, as:

$$F_y = \int_A \sigma_y dA = \sum_i \sum_j (\sigma_{y,i} \frac{A_{i,j}}{3}) \tag{15}$$

where $A_{i,j}$ is the area of the j-th triangle that has point i as one of its vertexes. As a special case, for regular triangular grids as shown in Fig.7, weights are the same and there is not much difference from the less generic case of rectangular structured grids. In our case, however, one might have arbitrary number of triangles and edges ending at the same point. This is useful, because in some cases the soil mesh comes in form of unstructured triangle meshes reconstructed from laser scanning etc.

4 Mesh refinement

An optional feature of our model is the ability to refine meshes in real time in order to increase or decrease the level of detail (LOD) of the soil.

It happens that very fine meshes are needed to capture the details of tire lugs, for example, but if an entire square kilometer of soil had to be discretized with such fine spacing of mesh points, the CPU time and the RAM requirements would be too high. Our solution is to add detail to the mesh as the tire proceeds on top of it.

We use the LEPP algorithm [17]. Figure 8 shows this algorithm in action, for a very simple case where the LOD of a single triangle t_0 must be adjusted to a given threshold.

The algorithm starts with an unstructured mesh, Fig. 8 a), with the assumption that the initial mesh does not have pathological or too stretched triangles (the LEPP algorithm does not change angles because it just splits the edges incrementally, so if an angle is too small in a given triangle, that angle will survive all the refinements).

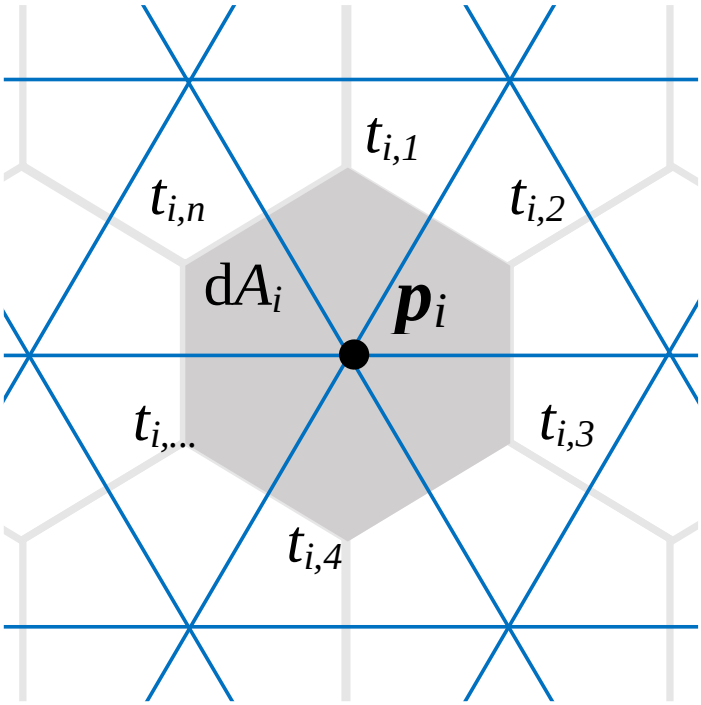

Figure 7: The i-th weight for quadrature of pressure integral (in case of regular triangle grids).

At each step, the algorithm splits the longest edge in the refined triangle, as in Fig. 8 b).

However, a caveat is used in the algorithm: the longest edge can be split only if it is the longest edge also for the neighborer triangle that shares it. For instance, after two refinements, one ends with t_0 being split in 4 triangles, but the two triangles on the lower diagonal cannot be split anymore without breaking the above mentioned rule. Thus, the LEPP algorithms proceeds by exploring the neighboring triangle(s) and see if the longest-edge rule can be applied; in Fig.8 c) one can see that this propagates the edge splitting to outer triangles, but the final result is well balanced and the LOD gradually increases from the outer areas to the initial t_0 triangle.

The LEPP algorithm can run in real time without much CPU overhead, it increases the LOD only for the triangles that are marked as "touching" as they have $\sigma > 0$, as shown in Fig. 9. The only requirement from the user side is a LOD threshold value, i.e. the maximum allowed length of edges in the contact area.

A similar strategy could be used to simplify unused soil back to the original LOD when the vehicle went far enough.

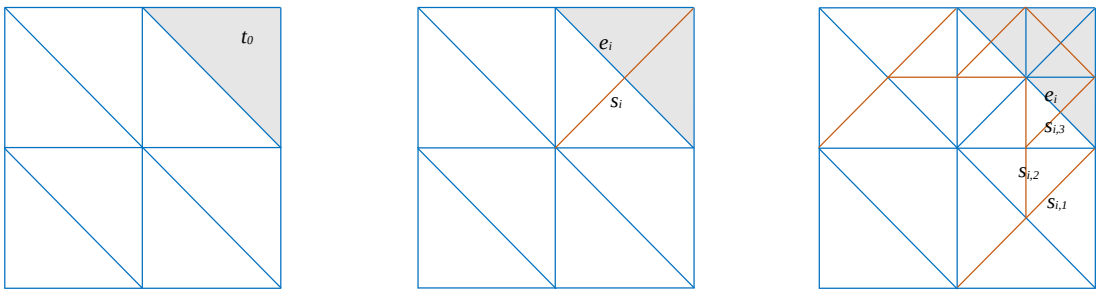

Figure 8: The LEPP algorithm for mesh refinement.

5 Conclusion

The extended SCM soil model provides a semi-empirical approach to the simulation of soft soil. It offers high speed of simulation and it is accurate enough for many scenarios. The new soil model, which is implemented in Chrono through the **DeformableTerrain** class, has the following attributes: it depends on few parameters (the same that are used in the Bekker-Wong model); it can generate 3D ruts on terrains of variable height; it takes into account multi-pass hardening when wheels generate intersecting ruts; it can work with irregular triangle-based terrain meshes; it supports an optional refinement of the terrain mesh to capture fine details like tire threads and lugs; and, it is compatible with deformable tires and generic shapes like obstacles, track shoes of tanks, etc.

On the downside, the new soil model cannot simulate lateral bulldozing effects like those happening when a tracked vehicle steers in-place and pushes material apart.

References

[1] Ali Azimi, Jozsef Kövecses, and Jorge Angeles. Wheel-soil interaction model for rover simulation based on plasticity theory. In *2011 IEEE/RSJ International Conference on Intelligent Robots and Systems*, pages 280–285. IEEE, 2011.

[2] Ali Azimi, József Kövecses, and Jorge Angeles. Wheel–soil interaction model for rover simulation and analysis using elastoplasticity theory. *IEEE Transactions on robotics*, 29(5):1271–1288, 2013.

[3] M.G. Bekker. *Theory of land locomotion: the mechanics of vehicle mobility*. University of Michigan Press, 1956.

[4] Liang Ding, Haibo Gao, Zongquan Deng, Keiji Nagatani, and Kazuya Yoshida. Experimental study and analysis on driving wheels performance for planetary exploration rovers moving in deformable soil. *Journal of Terramechanics*, 48(1):27–45, 2011.

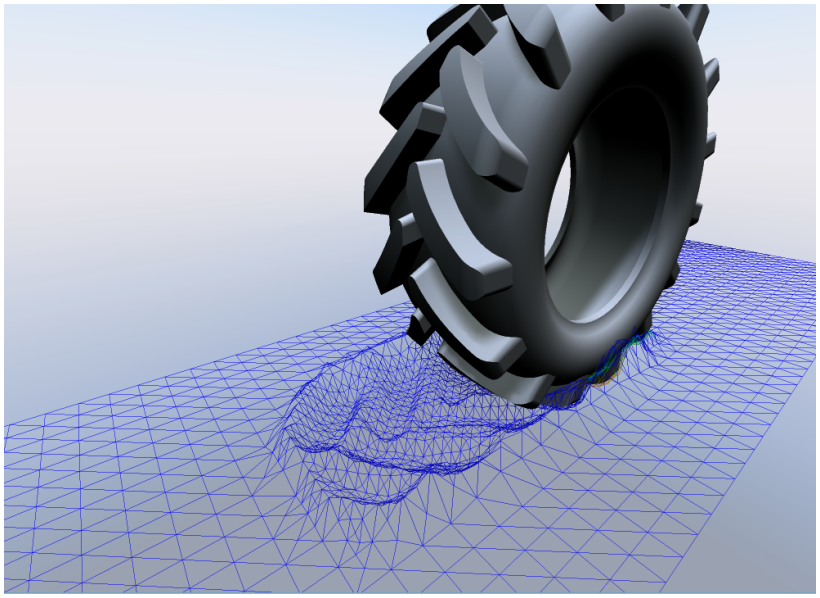

Figure 9: Automatic mesh refinement under the wheel footprint and in the surrounding region.

[5] Andreas Gibbesch and B Schafer. Multibody system modelling and simulation of planetary rover mobility on soft terrain. In *8th International Symposium on Artificial Intelligence, Robotics and Automation in Space (i-SAIRAS 2005), Munich, Germany, September*, pages 5–8, 2005.

[6] Karl Iagnemma, Shinwoo Kang, Hassan Shibly, and Steven Dubowsky. Online terrain parameter estimation for wheeled mobile robots with application to planetary rovers. *IEEE Transactions on Robotics*, 20(5):921–927, 2004.

[7] Genya Ishigami, Akiko Miwa, Keiji Nagatani, and Kazuya Yoshida. Terramechanics-based model for steering maneuver of planetary exploration rovers on loose soil. *Journal of Field robotics*, 24(3):233–250, 2007.

[8] Z Janosi and Ben Hanamoto. The analytical determination of drawbar pull as a function of slip for tracked vehicles in deformable soils. In *First International Conference on Terrain-Vehicle Systems, Turin, Italy*, 1961.

[9] Zhenzhong Jia, William Smith, and Huei Peng. Fast analytical models of wheeled locomotion in deformable terrain for mobile robots. *Robotica*, 31(01):35–53, 2013.

[10] Rainer Krenn and Andreas Gibbesch. Soft soil contact modeling technique for multibody system simulation. In *Trends in computational contact mechanics*, pages 135–155. Springer, 2011.

[11] Rainer Krenn, Andreas Gibbesch, and Gerd Hirzinger. Contact dynamics simulation of rover locomotion. *Proceedings of the 9th i-SAIRAS, Los Angeles, CA, USA*, 2008.

[12] Rainer Krenn and Gerd Hirzinger. Simulation of rover locomotion on sandy terrain-modeling, verification and validation. In *Proceedings of the 10th Workshop on ASTRA, Noordwijk, The Netherlands*, 2008.

[13] Daniel Melanz, Paramsothy Jayakumar, and Dan Negrut. Experimental validation of a differential variational inequality-based approach for handling friction and contact in vehicle/granular-terrain interaction. *Journal of Terramechanics*, 65:1–13, 2016.

[14] H Nakashima, H Fujii, A Oida, M Momozu, Y Kawase, H Kanamori, S Aoki, and T Yokoyama. Parametric analysis of lugged wheel performance for a lunar microrover by means of dem. *Journal of Terramechanics*, 44(2):153–162, 2007.

[15] H Nakashima and A Oida. Algorithm and implementation of soil–tire contact analysis code based on dynamic fe–de method. *Journal of Terramechanics*, 41(2):127–137, 2004.

[16] RD Nelson and ET Selig. Bulldozing resistance of plane blades in cohesionless soil. Technical report, SAE Technical Paper, 1964.

[17] María-Cecilia Rivara. Selective refinement/derefinement algorithms for sequences of nested triangulations. *International journal for numerical methods in Engineering*, 28(12):2889–2906, 1989.

[18] Bernd Schäfer, Andreas Gibbesch, Rainer Krenn, and Bernhard Rebele. Planetary rover mobility simulation on soft and uneven terrain. *Vehicle System Dynamics*, 48(1):149–169, 2010.

[19] C Senatore and KD Iagnemma. Direct shear behaviour of dry, granular soils for low normal stress with application to lightweight robotic vehicle modelling. In *Proceedings of the 17th International Conference on Terrain-Vehicle Systems ISTVS, Blacksburg, VA*, pages 1–11, 2011.

[20] C Senatore and C Sandu. Off-road tire modeling and the multi-pass effect for vehicle dynamics simulation. *Journal of Terramechanics*, 48(4):265–276, 2011.

[21] H Shibly, Karl Iagnemma, and S Dubowsky. An equivalent soil mechanics formulation for rigid wheels in deformable terrain, with application to planetary exploration rovers. *Journal of Terramechanics*, 42(1):1–13, 2005.

[22] William Smith, Daniel Melanz, Carmine Senatore, Karl Iagnemma, and Huei Peng. Comparison of discrete element method and traditional modeling methods for steady-state wheel-terrain interaction of small vehicles. *Journal of Terramechanics*, 56:61–75, 2014.

[23] Tamer M Wasfy, Hatem M Wasfy, and Jeanne M Peters. Coupled multibody dynamics and discrete element modeling of vehicle mobility on cohesive granular terrains. In *ASME 2014 International Design Engineering Technical Conferences and Computers and Information in Engineering Conference*, pages V006T10A050–V006T10A050. American Society of Mechanical Engineers, 2014.

[24] Jo Yung Wong et al. *Terramechanics and off-road vehicles.* Elsevier, 1989.

[25] Jo-Yung Wong and AR Reece. Prediction of rigid wheel performance based on the analysis of soil-wheel stresses part i. performance of driven rigid wheels. *Journal of Terramechanics*, 4(1):81–98, 1967.

[26] Kaiming Xia. Finite element modeling of tire/terrain interaction: Application to predicting soil compaction and tire mobility. *Journal of Terramechanics*, 48(2):113–123, 2011.

[27] Rui Zhang and Jianqiao Li. Simulation on mechanical behavior of cohesive soil by distinct element method. *Journal of Terramechanics*, 43(3):303–316, 2006.